CLUSTERING OF RED GALAXIES NEAR THE RADIO-LOUD QUASAR 1335.8+2834 AT z = 1.1 [1]

Toru Yamada, Ichi Tanaka

Astronomical Institute, Tohoku University, Aoba-ku, Sendai 980-77, Japan

Alfonso Aragón-Salamanca, Tadayuki Kodama

Institute of Astronomy, Madingley Road, Cambridge, CB3 0HA, UK

Kouji Ohta

Department of Astronomy, Kyoto University, Kyoto, 606-01, Japan

and

Nobuo Arimoto

Institute of Astronomy, University of Tokyo, Mitaka, Tokyo 181, Japan

Received _____; accepted _____

[1]Partly based on observations made with the University of Hawaii 2.2 m telescope, and the Isaac Newton Telescope, operated on the island of La Palma by the Royal Greenwich Observatory in the Spanish Observatorio del Roque de los Muchachos of the Instituto de Astrofísica de Canarias.

ABSTRACT

We have obtained new deep optical and near-infrared images of the field of the *radio-loud* quasar 1335.8+2834 at $z = 1.086$ where an excess in the surface number density of galaxies was reported by Hutchings et al. [AJ, 106, 1324] from optical data. We found a significant clustering of objects with very red optical-near infrared colors, $4 \lesssim R - K \lesssim 6$ and $3 \lesssim I - K \lesssim 5$ near the quasar. The colors and magnitudes of the reddest objects are consistent with those of old (12 Gyr old at $z = 0$) passively-evolving elliptical galaxies seen at $z = 1.1$, clearly defining a 'red envelope' like that found in galaxy clusters at similar or lower redshifts. This evidence strongly suggests that the quasar resides in a moderately-rich cluster of galaxies (richness-class ≥ 0). There is also a relatively large fraction of objects with moderately red colors ($3.5 < R - K < 4.5$) which have a distribution on the sky similar to that of the reddest objects. They may be interpreted as cluster galaxies with some recent or on-going star formation.

Subject headings: galaxies: evolution – galaxies: formation – galaxies: elliptical and lenticular, cD – quasars: general

1. Introduction

Clusters of galaxies from low to high redshift provide a unique opportunity to trace back the evolution of galaxies in dense environments. Detailed studies of elliptical galaxies in nearby and intermediate redshift clusters showed that their photometric properties are homogeneous and evolve only mildly with redshift at $z \lesssim 1$. This is consistent with the so-called 'passive evolution', namely the change of the photometric properties of elliptical galaxies by the aging of their stars only, with a formation epoch of at least ~ 10 Gyr ago (Bower, Lucey & Ellis 1992; Aragón-Salamanca et al. 1993; Ellis et al. 1997; Dickinson 1997b; Stanford, Eisenhardt, & Dickinson 1997). On the other hand, some S0 and spiral galaxies seem to experience faster evolution (e.g., Dressler et al. 1994; Dressler and Smail 1997). It is clear that pushing these studies to higher redshifts should provide stronger constraints on the epoch of cluster galaxy formation. Unfortunately, only a very limited number of clusters and cluster candidates are known beyond $z \simeq 1$ (Dickinson 1995; 1997b), and thus the identification of high-redshift clusters itself should be the next important step.

Near-infrared (NIR) observations are essential in identifying clusters of galaxies at $z \gtrsim 1$. It is known that old passively-evolving galaxies observed at high redshifts have very red optical-NIR colors (Aragón-Salamanca et al. 1993; Dickinson 1995; Yamada and Arimoto 1995), since their optical flux rapidly decreases as the 4000 Å break shifts toward longer wavelengths. For example, a 3 Gyr-old passively-evolving model galaxy observed at $z = 1$ has $I - K \sim 4$ which is redder than most galactic stars and most field galaxies. Therefore by selecting objects with red optical-NIR colors, the contrast between cluster and field galaxies will be very much enhanced if clusters are dominated by old galaxies.

It has been known for some time that radio-loud AGNs (both radio-galaxies and quasars) are frequently located in cluster environments (see, e.g., Yee & Green 1987; Ellingson, Yee & Green 1991; Dickinson 1995). Thus, targeted searches in the fields of

high redshift radio-loud AGN provide an efficient approach to the problem of finding the (probably) rare galaxy clusters at $z > 1$ (see Dickinson 1997c for a review).

In this *Letter* we report the clustering of very red objects in the vicinity of a quasar at $z = 1.1$ where some excess in the surface number density of galaxies had already been reported by Hutchings et al. (1993) based on their optical data. We obtained deeper R and I optical images and NIR K-band data of the region and confirmed the clustering of galaxies near the quasar; their optical-NIR colors and magnitudes are consistent with bright cluster galaxies formed at higher redshift and observed at $z = 1.1$. The cosmological parameters $H_0 = 50\,\mathrm{km\,s^{-1}\,Mpc^{-1}}$ and $q_0 = 0.5$ have been assumed.

2. Observations and data reduction

With the aim of identifying high redshift cluster galaxies with red optical-NIR colors, we have targeted the field around the radio-loud [2] quasar 1335.8+2834 at $z = 1.086$. Hutchings, Crampton & Persam (1993) found that the surface density of galaxies within $\sim 100''$ separation ($\sim 1\,\mathrm{Mpc}$ at $z = 1.1$) from the quasar is three times larger than the average density of their control fields. Using narrow-band images centered on the

[2]Hutchings et al. (1993) classified this quasar as radio quiet. However, a plausible radio counterpart with $S_{6\mathrm{cm}} = 55$ mJy exists at $(\alpha_{1950}, \delta_{1950}) = (13^h\,35^m\,47^s.8 \pm 1.2, +28^\circ\,20'\,19'' \pm 22)$ (Gregory and Condon 1991), while the quasar locates at $(13^h\,35^m\,48^s.39, +28^\circ\,20'\,24''.3)$ (Véron-Cetty and Véron 1996). We estimate that the logarithmic radio-optical luminosity ratio of the quasar is $\log(L_\nu^{6cm}/L_\nu^V) = 3.34$. Thus the 1335.8+2834 should be classified as radio-loud. In the recent VLA FIRST survey catalog (White et al. 1997), where the typical positional error is less than 1 arcsec, there is a radio source at $(13^h\,35^m\,48^s.409, +28^\circ\,20'\,22''.61)$.

[OII]λ3727Å line redshifted to $z = 1.086$, they also found several emission-line galaxies near the quasar, suggesting the excess density is associated with the quasar redshift.

Optical images were obtained with the Isaac Newton Telescope at la Palma on the 28th of February, 1995. A TEK 1024×1024 CCD with a projected pixel size of 0.59 arcsec was used. The weather conditions were mostly photometric. Total exposures of 8100 sec in the R band and 7500 sec in the I band were gathered, subdivided in 900 or 600 sec sub-exposures. The FWHM sizes of the stars were typically 1.5 (R) and 1.8 (I) arcsec. The frames were bias-subtracted, flat-fielded and median-stacked in the usual manner.

The K-band images were obtained with the University of Hawaii 2.2m telescope equipped with the QUIRC camera on the 29th of February, 1996. The detector was the 1024×1024 HgCdTe array with a projected pixel size of 0.18 arcsec. Since the field of view of this camera ($3 \times 3\,\mathrm{arcmin}^2$) is smaller than that of the optical CCD ($7 \times 7\,\mathrm{arcmin}^2$), we covered only the field which contains the region where the surface density had been evaluated to be high from the optical data. In this letter, we concentrate mainly on the properties of the objects contained within the K-band field. The net exposure time of the K-band image is 6480 sec, subdivided in many 180 sec dis-registered exposures. The FWHM size of the stellar images was 0.9 arcsec. Flat-field frames were built using a running median of $\simeq 10$ images in a time sequence. The flat-fielded images were then median-stacked and a constant sky value was subtracted. The data reduction was done with IRAF.

Object detection was carried out using FOCAS (Jarvis and Tyson 1981) with a detection threshold of 2.5σ of the sky fluctuations per pixel. A minimum of $\sim (FWHM)^2$ connecting pixels above the threshold was required for detection. Landolt (1992) standards in the R and I bands, and UKIRT bright standards in K were used for photometric calibration, yielding zero-point errors smaller than 0.1 mag. We measured the colors of the objects within a fixed aperture with a diameter of 3.6 arcsec, twice the FWHM seeing in

the I band image (the worse case), after correcting the seeing differences among the images. The APPHOT task in the IRAF was used for the photometry. Total magnitudes were also estimated using template growth curves determined from 10 isolated galaxies in the field.

The source detection is complete for objects brighter than 24.5, 23.5, and 20.0 magnitudes in R, I, and K respectively. These limits were estimated from the turn-off of the number counts in the 'field region' (western half of the K-band image), which avoids the region of the cluster candidate (see ahead). The counts are consistent, within $\simeq 1\sigma$, with published field number counts (e.g., Smail et al. 1995; Djorgovski et al. 1995). The internal photometric errors in the aperture magnitudes were evaluated using the photon count statistics and also by changing the sky regions in the local sky subtraction procedure. Typical errors are ~ 0.1 mag in R and ~ 0.15 mag in I and K at the completeness limits. The error in the K-band total magnitude (used in the color-magnitude diagram below) is estimated to be ~ 0.35 mag at $K \sim 20$ mag, where the uncertainties in our growth-curve-fitting procedure have been taken into account.

3. The spatial distribution and colors of the galaxies

Figure 1 shows the three-color image of the K-band field, and figure 2a shows the distribution of the objects detected in the K-band image. Objects with different colors are shown as different symbols. An excess in the number density of faint objects near the quasar (denoted by 'QSO') is seen. Hutchings et al. (1993) divided the image into cells and found a 3.5σ surface density excess in the number of objects in a $100 \times 100\,\mathrm{arcsec}^2$ region centered on the quasar. We made a similar analysis on our R and I optical images and found the excess surface density in a similar region to be 3σ above the counts of the surrounding field. Moreover, red objects are seen much more frequently in the eastern (left) half of the image near the quasar. The color of most objects in the western side of the field is $R - K \lesssim 3.5$

(see below). It is clear that objects with red optical-NIR colors are responsible for most of the excess in the number density. Since stars earlier than M3V have colors $R-K \lesssim 3.5$ (Johnson 1966; Bessell 1990), most of these red objects are probably galaxies (see figure 4). An un-evolved elliptical galaxy (the reddest case for a galaxy without extinction) has $R-K \sim 3.5$ at $z \sim 0.4$, thus these red objects are probably galaxies at higher redshifts.

A fairly bright galaxy near the quasar (G1 in Figures 1 and 2) has $K = 17.3$, $R-K = 5.7$, and $I-K = 4.3$, which agree very well with the expectations for a brightest cluster galaxy at $z \sim 1.1$ (Aragón-Salamanca et al 1993). A closer look at the spatial distribution of the overdensity indicates that the contrast is maximised when G1 is taken as the center, instead of the quasar. Figure 2b shows the surface-density-contrast profile, centered on G1, of all the objects detected in the K band as well as those with $R-K > 3.5$. The excess surface density of K-band detected objects in a 100 arcsec box centered on G1 is 6σ above the counts of the surrounding field, which is significantly above that found in the optical images. Moreover, if we consider only the red objects, the contrast of the putative cluster is significantly enhanced to $\simeq 10\sigma$ above the field counts, which clearly indicates that the use of optical-NIR colors is a powerful technique to identify high-redshift clusters.

The size of the region with the excess density is ~ 1 arcmin in diameter, corresponding to $\sim 0.5\,\mathrm{Mpc}$ at $z = 1.1$, which is consistent with that expected for a rich galaxy cluster. If we count all the galaxies with $R-K > 3.5$ as cluster members, nearly 30 galaxies remain after correcting for field contamination in this color range. This roughly corresponds to the Abell richness class 0. This could be a lower-limit for the cluster richness since we have only counted the red objects as cluster members. A more accurate estimate of the richness is not possible without galaxy redshifts.

Figure 3 shows the $R-K$ vs K color-magnitude diagram for the objects in the K-band field. We tentatively define the 'cluster region' as the eastern half of the field, and show

the objects in this area with filled circles. The color distributions in the two regions are very different. There are 37 galaxies with $3.5 < R - K < 6$ and $17 < K < 19$ in the eastern 'cluster region' but only 6 such objects in the western 'field' region. In the cluster region, there is a group of objects with similar colors and magnitudes, $4.5 < R - K < 6$ and $K = 17$–19 mag. They are consistent with a homogeneous population of galaxies seen at a similar redshift, which suggests that the clustering is probably real. These objects have $I - K \gtrsim 3$. The $I - K$ color is very redshift-sensitive at $z \sim 1$ due to the fact that the 4000 Å break is located near or just inside the I band at this redshift. Thus, the red $I - K$ colors strongly suggest that these objects are old galaxies at $z \gtrsim 1$. For comparison, on Figure 3 we also plot the model colors and magnitudes of passively-evolving elliptical galaxies calculated with the models introduced by Kodama and Arimoto (1997). The model parameters are chosen so that the color-magnitude relation at $z = 0$ (interpreted as a mass-metallicity sequence) agrees with that of the Coma cluster (Bower et al. 1992). The color and luminosity evolution predicted by such models agrees very well with the observed one for cluster ellipticals (see Kodama and Arimoto 1997). The solid lines indicate the expected colors of passively-evolving model galaxies with $M_V = -22.0$ and -18.5 mag at $z = 0$, which are formed at $z_f = 4.5$ ($t_{age} = 12$ Gyr at $z = 0$). Tilted straight lines indicate the expected color-magnitude relation at different redshifts (see caption). The colors of the reddest galaxies in the complete sample are consistent with passively-evolving old galaxies observed at $z = 1.1$. They define a 'red envelope' as expected if they are the oldest cluster galaxies at this redshift, although a clear color-magnitude sequence is not seen.

The color-magnitude diagram also reveals a significant fraction of objects with $3.5 < R - K < 4.5$ and $K \sim 17 - 19$. Since their color distribution seems somewhat separated from the redder galaxies, it is possible that these objects belong to a different system at lower redshift ($z \sim 0.6$). However, the sky distribution of these moderately red objects is similar to that of the reddest objects (cf. Figure 2a), so it is possible that they

are in the same system. Without redshifts, these to possibilities cannot be discriminated.

Figure 4 shows the two-color diagram for the 'cluster' (west half) and 'field' (east half) galaxies. The solid line shows the colors of elliptical galaxies observed at various redshifts derived from the same models as in Figure 3, representing the expected locus of the reddest galaxies observed at any redshift in the absence of reddening. It is clear that the reddest galaxies in both $R-K$ and $R-I$ are compatible with being passively-evolving cluster ellipticals at $z = 1.1$. On the other hand, there is a number of galaxies with moderately red $R-K$ color ($3.5 \lesssim R-K \lesssim 5$) and bluer $R-I$ colors. Hutchings et al. (1993) had also noticed the bimodal distribution of $R-I$ colors in the excess-density region, which is not seen in their control field. If they are cluster members, their bluer optical colors would suggest a certain amount of current or recent star forming activity.

4. Discussion and Conclusions

We have found significant clustering of galaxies with very red optical-NIR colors near the radio-loud quasar 1335.8+2834 at $z = 1.1$. The reddest objects ($4.5 \lesssim R-K \lesssim 6$) are responsible for nearly half of the surface density excess, and their colors and magnitudes are consistent with those of passively-evolving old galaxies seen at $z \sim 1.1$. If they are at the quasar redshift, galaxy evolution models suggest that in the absence of reddening the reddest objects are already $\sim$ 2–4 Gyr old. The range of colors displayed by the galaxies can be readily explained by the presence of some field galaxies at a variety of redshifts and by cluster galaxies with a variety of star formation histories such as disk galaxies formed a few Gyr before $z = 1.1$, or old galaxies with young bursts of star formation. Redshifts and morphologies are needed to study the evolutionary properties of the galaxies in detail.

Other examples of clustering of red galaxies near a radio-loud object at comparable

redshifts have been found by Dickinson and his collaborators (Dickinson 1995; 1997a). They observed the fields of powerful radio galaxies at intermediate and high redshifts with a similar optical and NIR imaging strategy. The cluster around 3C 324 is their most outstanding case. Redshifts for a few hundred objects confirmed a cluster at $z = 1.21$ associated with 3C 324, although many interlopers in another group or cluster at $z = 1.15$ were also found. A similar contamination by a group or cluster at a slightly different redshift cannot be excluded in the case of 1335.8+2834 without extensive redshift data.

Hintzen, Romanishin & Valdes (1991) have also found significant clustering of galaxies around $z = 0.9$–1.5 radio-loud quasars. The galaxies responsible for the excess they detected seemed to be more luminous in the observed R-band than present-day brightest cluster galaxies. However, the galaxies responsible for the excess we have found in the field of 1335.8+2834 do not seem to be over-luminous in the K-band. Since the observed R-band samples ultraviolet light at these redshifts, evolutionary effects such as the presence of moderate amounts of young stars can boost up the observed flux considerably, while the NIR should show significantly milder evolutionary effects.

Excess in the galaxy number density has also been found for higher-redshift quasars or radio galaxies (Dressler et al. 1993, 1994; Hutchings 1995; Pascarelle et al. 1996). These authors claim that the excess galaxies are small compact objects which may be the 'building blocks' of today's luminous galaxies. In contrast, many of the galaxies found near 1335.8+2834 are fairly luminous ($\gtrsim 0.5L_*$). Similarly, an excess of $\sim L_*$ galaxies was found near radio-loud quasars at $z \sim 2$ by Aragón-Salamanca, Ellis, and O'Brien (1996). The situation is therefore not clear, and a systematic study of the fields of a large well-defined sample of known high redshift objects is clearly needed.

In summary, we have shown that the combination of deep optical and NIR imaging is a very powerful tool in revealing high redshift clusters of galaxies and/or their progenitors. Such clusters can provide samples of high redshift galaxies for evolutionary studies at

large look-back times, which can greatly contribute to our knowledge of galaxy formation and evolution at very early epochs. While this kind of study is very successful at finding candidate clusters, redshifts and morphologies will be ultimately needed.

This work was partially supported by a grant-in-aid for Scientific Research of the Japanese Ministry of Education, Science, Sports and Culture (No.07041104 and No.08740181). Part of this work was also supported by the Foundation for the Promotion of Astronomy of Japan. TY was a Special Post-Doctoral Researcher of the Institute of Physical and Chemical Research (RIKEN) and a part of this work was supported by this institute. AAS acknowledges generous financial support from the Royal Society and the Particle Physics and Astronomy Research Council. TK thanks to the Japan Society for the Promotion of Science Postdoctoral Fellowships for Research Abroad. KO was a visiting astronomer of the Institute for Astronomy, University of Hawaii and thanks their hospitality during his stay.

REFERENCES

Aragón-Salamanca, A., Ellis, R. S., Couch, W. J., & Carter, D. 1993, MNRAS, 262, 764

Aragón-Salamanca, A., Ellis, R.S. & O'Brien, K.S. 1996, MNRAS, 281, 945

Bessell, M. S. 1990, PASP, 102, 1181

Bower, R. G., Lucey, J. R., & Ellis, R. S. 1992, MNRAS, 254, 601

Dickinson, M. 1995, in ASP Conf. Ser. Vol.86 Fresh View of Elliptical Galaxies, eds. A. Buzzoni, A. Renzini, & A. Serrano, p.283

Dickinson, M. 1997a, in HST and the High Redshift Universe, ed. N. Tanvir, A. Aragón-Salamanca, and J.V. Wall, (Singapore: World Scientific), p.207

Dickinson, M. 1997b, in Galaxy Scaling Relations: Origins, Evolution and Applications, ed. L. da Costa (Springer-Verlag), in press, *astro-ph/9703035*

Dickinson, M. 1997c, in The Early Universe with the VLT, ed. J. Bergeron, (Springer-Verlag), p.274

Djorgovski, S. G., et al. 1995, ApJ, 438, L13

Dressler, A., & Smail, I. 1997, in HST and the High Redshift Universe, ed. N. Tanvir, A. Aragón-Salamanca, and J.V. Wall, (Singapore: World Scientific), p.185

Dressler, A., Oemler, A., Gunn, J., & Butcher, H. 1993, ApJ, 404, L45

Dressler, A., Oemler, A., Butcher, H., & Gunn, J. 1994, ApJ, 435, L23

Ellingson, E., & Yee, H. K. C. 1991, ApJ, 371, 49

Ellingson, E., Yee, H.K.C. & Green, R.F. 1991, ApJ, 371, 36

Ellis, R. S., Smail, I., Dressler, A., Couch, W. J., Oemler, A., Butcher, H., & Sharples, R. M. 1997, ApJ, 483, 582

Gregory, P.C., & Condon, J.J. 1991, ApJS, 75, 1011

Hintzen P., Romanishin W., & Valdes, F. 1991, ApJ, 366, 7

Hutchings, J. B. 1995, AJ, 110, 994

Hutchings, J. B., Crampton, D., & Persram, D. 1993, AJ, 106, 1324

Hutchings, J. B., Crampton, D., & Johnson, A. 1995, AJ, 109, 73

Jarvis, J. F., & Tyson, J. A. 1981, AJ, 86, 476

Johnson, H.L. 1966, ARA&A, 4, 193

Kodama, T., & Arimoto,N. 1997, A&A, 320, 41

Landolt, A. U. 1992, AJ, 104, 340

Pascarelle, S. M., Windhorst, R. A., Keel, W. C., & Odewahn, S. C. 1996, Nature, 383, 45

Smail, I., Hogg, D. W., Yan, L., & Cohen, J. G. 1995, ApJ, 449, L105

Stanford, S. A., Eisenhardt, P. R. M., & Dickinson, M. 1995, ApJ, 450, 512

Stanford, S.A., Eisenhardt, P.R.M., and Dickinson, M. 1997, ApJ, submitted

Véron-Cetty, M.-P. & Véron, P. 1996, A&AS, 115, 97

White, R. L., Becker, R. H., Helfand, D. J., Gregg, M. D. 1997, ApJ, 475, 479

Yamada T., & Arimoto, N. 1995, in IAU symp. No.171, New Light on Galaxy Evolution, eds. R. Bender, & R. L. Davies, p.472

Yee, H. K. C. & Green, R. F. 1987, ApJ, 319, 28

Fig. 1.— RIK three color image of the field near the radio-loud quasar 1335.8+2834 at $z = 1.086$ (QSO). North is up, East is left. The field is 160 arcsec on each side, which corresponds to $0.62\,h^{-1}$Mpc for q_0=0.5.

Fig. 2.— **(a)** Distribution of the K-selected objects on the sky. Scale and orientation as in Figure 1. Objects in different color ranges are shown as different symbols. **(b)** Surface-density-contrast profile, $(\Sigma(\theta) - \langle\Sigma\rangle)/\langle\Sigma\rangle$, for all the K-selected objects centered on galaxy G1 (dash-dotted line) and for the objects with $R - K \geq 3.5$ (solid line). The average field number densities are the values obtained at the western half of the image avoiding the cluster region.

Fig. 3.— $R - K$ vs. K color-magnitude diagram of the complete photometric sample. The completeness limits are shown by the dashed lines. The objects in the putative cluster region, namely the eastern half of the frame, are shown as filled circles. Those in the western half are shown as open circles. The predicted colors and magnitudes of model galaxies with $M_V = -22.0$ and -18.5 mag at $z = 0$, formed at $z_f = 4.5$ are shown as solid lines. Tilted dash-dotted lines indicate the expected color-magnitude relation observed at $z = 0.2$, 0.6, 0.9, 1.1, and 1.4, which correspond to galaxy ages of 8.9, 5.4, 3.9, 3.2, and 2.5 Gyr, respectively (computed from the models of Kodama and Arimoto 1997).

Fig. 4.— $R - K$ vs. $R - I$ color-color diagram for the complete sample. Symbols are as in Figure 3. The solid line indicates the predicted colors of model galaxies with $M_V = -20.5$ mag at $z = 0$ observed at various redshifts derived from the same models as in Figure 3. The labeled crosses indicate the observed redshifts. Colors of dwarf (G0V–M5V) and giant (G5III–M6III) stars (Johnson 1966; Bessell 1990) are also plotted for reference (dashed lines).

This manuscript was prepared with the AAS LaTeX macros v4.0.

CLUSTERING OF RED GALAXIES NEAR THE RADIO-LOUD QUASAR 1335.8+2834 AT z = 1.1 [1]

Toru Yamada, Ichi Tanaka

Astronomical Institute, Tohoku University, Aoba-ku, Sendai 980-77, Japan

Alfonso Aragón-Salamanca, Tadayuki Kodama

Institute of Astronomy, Madingley Road, Cambridge, CB3 0HA, UK

Kouji Ohta

Department of Astronomy, Kyoto University, Kyoto, 606-01, Japan

and

Nobuo Arimoto

Institute of Astronomy, University of Tokyo, Mitaka, Tokyo 181, Japan

Received _____; accepted _____

[1]Partly based on observations made with the University of Hawaii 2.2 m telescope, and the Isaac Newton Telescope, operated on the island of La Palma by the Royal Greenwich Observatory in the Spanish Observatorio del Roque de los Muchachos of the Instituto de Astrofísica de Canarias.

ABSTRACT

We have obtained new deep optical and near-infrared images of the field of the *radio-loud* quasar 1335.8+2834 at $z = 1.086$ where an excess in the surface number density of galaxies was reported by Hutchings et al. [AJ, 106, 1324] from optical data. We found a significant clustering of objects with very red optical-near infrared colors, $4 \lesssim R - K \lesssim 6$ and $3 \lesssim I - K \lesssim 5$ near the quasar. The colors and magnitudes of the reddest objects are consistent with those of old (12 Gyr old at $z = 0$) passively-evolving elliptical galaxies seen at $z = 1.1$, clearly defining a 'red envelope' like that found in galaxy clusters at similar or lower redshifts. This evidence strongly suggests that the quasar resides in a moderately-rich cluster of galaxies (richness-class ≥ 0). There is also a relatively large fraction of objects with moderately red colors ($3.5 < R - K < 4.5$) which have a distribution on the sky similar to that of the reddest objects. They may be interpreted as cluster galaxies with some recent or on-going star formation.

Subject headings: galaxies: evolution – galaxies: formation – galaxies: elliptical and lenticular, cD – quasars: general

1. Introduction

Clusters of galaxies from low to high redshift provide a unique opportunity to trace back the evolution of galaxies in dense environments. Detailed studies of elliptical galaxies in nearby and intermediate redshift clusters showed that their photometric properties are homogeneous and evolve only mildly with redshift at $z \lesssim 1$. This is consistent with the so-called 'passive evolution', namely the change of the photometric properties of elliptical galaxies by the aging of their stars only, with a formation epoch of at least ~ 10 Gyr ago (Bower, Lucey & Ellis 1992; Aragón-Salamanca et al. 1993; Ellis et al. 1997; Dickinson 1997b; Stanford, Eisenhardt, & Dickinson 1997). On the other hand, some S0 and spiral galaxies seem to experience faster evolution (e.g., Dressler et al. 1994; Dressler and Smail 1997). It is clear that pushing these studies to higher redshifts should provide stronger constraints on the epoch of cluster galaxy formation. Unfortunately, only a very limited number of clusters and cluster candidates are known beyond $z \simeq 1$ (Dickinson 1995; 1997b), and thus the identification of high-redshift clusters itself should be the next important step.

Near-infrared (NIR) observations are essential in identifying clusters of galaxies at $z \gtrsim 1$. It is known that old passively-evolving galaxies observed at high redshifts have very red optical-NIR colors (Aragón-Salamanca et al. 1993; Dickinson 1995; Yamada and Arimoto 1995), since their optical flux rapidly decreases as the 4000 Å break shifts toward longer wavelengths. For example, a 3 Gyr-old passively-evolving model galaxy observed at $z = 1$ has $I - K \sim 4$ which is redder than most galactic stars and most field galaxies. Therefore by selecting objects with red optical-NIR colors, the contrast between cluster and field galaxies will be very much enhanced if clusters are dominated by old galaxies.

It has been known for some time that radio-loud AGNs (both radio-galaxies and quasars) are frequently located in cluster environments (see, e.g., Yee & Green 1987; Ellingson, Yee & Green 1991; Dickinson 1995). Thus, targeted searches in the fields of

high redshift radio-loud AGN provide an efficient approach to the problem of finding the (probably) rare galaxy clusters at $z > 1$ (see Dickinson 1997c for a review).

In this *Letter* we report the clustering of very red objects in the vicinity of a quasar at $z = 1.1$ where some excess in the surface number density of galaxies had already been reported by Hutchings et al. (1993) based on their optical data. We obtained deeper R and I optical images and NIR K-band data of the region and confirmed the clustering of galaxies near the quasar; their optical-NIR colors and magnitudes are consistent with bright cluster galaxies formed at higher redshift and observed at $z = 1.1$. The cosmological parameters $H_0 = 50\,\mathrm{km\,s^{-1}\,Mpc^{-1}}$ and $q_0 = 0.5$ have been assumed.

2. Observations and data reduction

With the aim of identifying high redshift cluster galaxies with red optical-NIR colors, we have targeted the field around the radio-loud [2] quasar 1335.8+2834 at $z = 1.086$. Hutchings, Crampton & Persam (1993) found that the surface density of galaxies within $\sim 100''$ separation ($\sim 1\,\mathrm{Mpc}$ at $z = 1.1$) from the quasar is three times larger than the average density of their control fields. Using narrow-band images centered on the

[2]Hutchings et al. (1993) classified this quasar as radio quiet. However, a plausible radio counterpart with $S_{6\mathrm{cm}} = 55$ mJy exists at $(\alpha_{1950}, \delta_{1950}) = (13^h\,35^m\,47^s.8 \pm 1.2, +28^\circ\,20'\,19'' \pm 22)$ (Gregory and Condon 1991), while the quasar locates at $(13^h\,35^m\,48^s.39, +28^\circ\,20'\,24''.3)$ (Véron-Cetty and Véron 1996). We estimate that the logarithmic radio-optical luminosity ratio of the quasar is $\log(L_\nu^{6cm}/L_\nu^V) = 3.34$. Thus the 1335.8+2834 should be classified as radio-loud. In the recent VLA FIRST survey catalog (White et al. 1997), where the typical positional error is less than 1 arcsec, there is a radio source at $(13^h\,35^m\,48^s.409, +28^\circ\,20'\,22''.61)$.

[OII]λ3727Å line redshifted to $z = 1.086$, they also found several emission-line galaxies near the quasar, suggesting the excess density is associated with the quasar redshift.

Optical images were obtained with the Isaac Newton Telescope at la Palma on the 28th of February, 1995. A TEK 1024×1024 CCD with a projected pixel size of 0.59 arcsec was used. The weather conditions were mostly photometric. Total exposures of 8100 sec in the R band and 7500 sec in the I band were gathered, subdivided in 900 or 600 sec sub-exposures. The FWHM sizes of the stars were typically 1.5 (R) and 1.8 (I) arcsec. The frames were bias-subtracted, flat-fielded and median-stacked in the usual manner.

The K-band images were obtained with the University of Hawaii 2.2m telescope equipped with the QUIRC camera on the 29th of February, 1996. The detector was the 1024×1024 HgCdTe array with a projected pixel size of 0.18 arcsec. Since the field of view of this camera ($3 \times 3\,\mathrm{arcmin}^2$) is smaller than that of the optical CCD ($7 \times 7\,\mathrm{arcmin}^2$), we covered only the field which contains the region where the surface density had been evaluated to be high from the optical data. In this letter, we concentrate mainly on the properties of the objects contained within the K-band field. The net exposure time of the K-band image is 6480 sec, subdivided in many 180 sec dis-registered exposures. The FWHM size of the stellar images was 0.9 arcsec. Flat-field frames were built using a running median of $\simeq 10$ images in a time sequence. The flat-fielded images were then median-stacked and a constant sky value was subtracted. The data reduction was done with IRAF.

Object detection was carried out using FOCAS (Jarvis and Tyson 1981) with a detection threshold of 2.5σ of the sky fluctuations per pixel. A minimum of $\sim (FWHM)^2$ connecting pixels above the threshold was required for detection. Landolt (1992) standards in the R and I bands, and UKIRT bright standards in K were used for photometric calibration, yielding zero-point errors smaller than 0.1 mag. We measured the colors of the objects within a fixed aperture with a diameter of 3.6 arcsec, twice the FWHM seeing in

the I band image (the worse case), after correcting the seeing differences among the images. The APPHOT task in the IRAF was used for the photometry. Total magnitudes were also estimated using template growth curves determined from 10 isolated galaxies in the field.

The source detection is complete for objects brighter than 24.5, 23.5, and 20.0 magnitudes in R, I, and K respectively. These limits were estimated from the turn-off of the number counts in the 'field region' (western half of the K-band image), which avoids the region of the cluster candidate (see ahead). The counts are consistent, within $\simeq 1\sigma$, with published field number counts (e.g., Smail et al. 1995; Djorgovski et al. 1995). The internal photometric errors in the aperture magnitudes were evaluated using the photon count statistics and also by changing the sky regions in the local sky subtraction procedure. Typical errors are ~ 0.1 mag in R and ~ 0.15 mag in I and K at the completeness limits. The error in the K-band total magnitude (used in the color-magnitude diagram below) is estimated to be ~ 0.35 mag at $K \sim 20$ mag, where the uncertainties in our growth-curve-fitting procedure have been taken into account.

3. The spatial distribution and colors of the galaxies

Figure 1 shows the three-color image of the K-band field, and figure 2a shows the distribution of the objects detected in the K-band image. Objects with different colors are shown as different symbols. An excess in the number density of faint objects near the quasar (denoted by 'QSO') is seen. Hutchings et al. (1993) divided the image into cells and found a 3.5σ surface density excess in the number of objects in a $100 \times 100\,\mathrm{arcsec}^2$ region centered on the quasar. We made a similar analysis on our R and I optical images and found the excess surface density in a similar region to be 3σ above the counts of the surrounding field. Moreover, red objects are seen much more frequently in the eastern (left) half of the image near the quasar. The color of most objects in the western side of the field is $R - K \lesssim 3.5$

(see below). It is clear that objects with red optical-NIR colors are responsible for most of the excess in the number density. Since stars earlier than M3V have colors $R-K \lesssim 3.5$ (Johnson 1966; Bessell 1990), most of these red objects are probably galaxies (see figure 4). An un-evolved elliptical galaxy (the reddest case for a galaxy without extinction) has $R-K \sim 3.5$ at $z \sim 0.4$, thus these red objects are probably galaxies at higher redshifts.

A fairly bright galaxy near the quasar (G1 in Figures 1 and 2) has $K = 17.3$, $R-K = 5.7$, and $I-K = 4.3$, which agree very well with the expectations for a brightest cluster galaxy at $z \sim 1.1$ (Aragón-Salamanca et al 1993). A closer look at the spatial distribution of the overdensity indicates that the contrast is maximised when G1 is taken as the center, instead of the quasar. Figure 2b shows the surface-density-contrast profile, centered on G1, of all the objects detected in the K band as well as those with $R-K > 3.5$. The excess surface density of K-band detected objects in a 100 arcsec box centered on G1 is 6σ above the counts of the surrounding field, which is significantly above that found in the optical images. Moreover, if we consider only the red objects, the contrast of the putative cluster is significantly enhanced to $\simeq 10\sigma$ above the field counts, which clearly indicates that the use of optical-NIR colors is a powerful technique to identify high-redshift clusters.

The size of the region with the excess density is ~ 1 arcmin in diameter, corresponding to $\sim 0.5\,\mathrm{Mpc}$ at $z = 1.1$, which is consistent with that expected for a rich galaxy cluster. If we count all the galaxies with $R-K > 3.5$ as cluster members, nearly 30 galaxies remain after correcting for field contamination in this color range. This roughly corresponds to the Abell richness class 0. This could be a lower-limit for the cluster richness since we have only counted the red objects as cluster members. A more accurate estimate of the richness is not possible without galaxy redshifts.

Figure 3 shows the $R-K$ vs K color-magnitude diagram for the objects in the K-band field. We tentatively define the 'cluster region' as the eastern half of the field, and show

the objects in this area with filled circles. The color distributions in the two regions are very different. There are 37 galaxies with $3.5 < R-K < 6$ and $17 < K < 19$ in the eastern 'cluster region' but only 6 such objects in the western 'field' region. In the cluster region, there is a group of objects with similar colors and magnitudes, $4.5 < R-K < 6$ and $K = 17$–19 mag. They are consistent with a homogeneous population of galaxies seen at a similar redshift, which suggests that the clustering is probably real. These objects have $I-K \gtrsim 3$. The $I-K$ color is very redshift-sensitive at $z \sim 1$ due to the fact that the 4000 Å break is located near or just inside the I band at this redshift. Thus, the red $I-K$ colors strongly suggest that these objects are old galaxies at $z \gtrsim 1$. For comparison, on Figure 3 we also plot the model colors and magnitudes of passively-evolving elliptical galaxies calculated with the models introduced by Kodama and Arimoto (1997). The model parameters are chosen so that the color-magnitude relation at $z = 0$ (interpreted as a mass-metallicity sequence) agrees with that of the Coma cluster (Bower et al. 1992). The color and luminosity evolution predicted by such models agrees very well with the observed one for cluster ellipticals (see Kodama and Arimoto 1997). The solid lines indicate the expected colors of passively-evolving model galaxies with $M_V = -22.0$ and -18.5 mag at $z = 0$, which are formed at $z_f = 4.5$ ($t_{age} = 12$ Gyr at $z = 0$). Tilted straight lines indicate the expected color-magnitude relation at different redshifts (see caption). The colors of the reddest galaxies in the complete sample are consistent with passively-evolving old galaxies observed at $z = 1.1$. They define a 'red envelope' as expected if they are the oldest cluster galaxies at this redshift, although a clear color-magnitude sequence is not seen.

The color-magnitude diagram also reveals a significant fraction of objects with $3.5 < R-K < 4.5$ and $K \sim 17-19$. Since their color distribution seems somewhat separated from the redder galaxies, it is possible that these objects belong to a different system at lower redshift ($z \sim 0.6$). However, the sky distribution of these moderately red objects is similar to that of the reddest objects (cf. Figure 2a), so it is possible that they

are in the same system. Without redshifts, these to possibilities cannot be discriminated.

Figure 4 shows the two-color diagram for the 'cluster' (west half) and 'field' (east half) galaxies. The solid line shows the colors of elliptical galaxies observed at various redshifts derived from the same models as in Figure 3, representing the expected locus of the reddest galaxies observed at any redshift in the absence of reddening. It is clear that the reddest galaxies in both $R-K$ and $R-I$ are compatible with being passively-evolving cluster ellipticals at $z = 1.1$. On the other hand, there is a number of galaxies with moderately red $R-K$ color ($3.5 \lesssim R-K \lesssim 5$) and bluer $R-I$ colors. Hutchings et al. (1993) had also noticed the bimodal distribution of $R-I$ colors in the excess-density region, which is not seen in their control field. If they are cluster members, their bluer optical colors would suggest a certain amount of current or recent star forming activity.

4. Discussion and Conclusions

We have found significant clustering of galaxies with very red optical-NIR colors near the radio-loud quasar 1335.8+2834 at $z = 1.1$. The reddest objects ($4.5 \lesssim R-K \lesssim 6$) are responsible for nearly half of the surface density excess, and their colors and magnitudes are consistent with those of passively-evolving old galaxies seen at $z \sim 1.1$. If they are at the quasar redshift, galaxy evolution models suggest that in the absence of reddening the reddest objects are already $\sim$ 2–4 Gyr old. The range of colors displayed by the galaxies can be readily explained by the presence of some field galaxies at a variety of redshifts and by cluster galaxies with a variety of star formation histories such as disk galaxies formed a few Gyr before $z = 1.1$, or old galaxies with young bursts of star formation. Redshifts and morphologies are needed to study the evolutionary properties of the galaxies in detail.

Other examples of clustering of red galaxies near a radio-loud object at comparable redshifts have been found by Dickinson and his collaborators (Dickinson 1995; 1997a).

They observed the fields of powerful radio galaxies at intermediate and high redshifts with a similar optical and NIR imaging strategy. The cluster around 3C 324 is their most outstanding case. Redshifts for a few hundred objects confirmed a cluster at $z = 1.21$ associated with 3C 324, although many interlopers in another group or cluster at $z = 1.15$ were also found. A similar contamination by a group or cluster at a slightly different redshift cannot be excluded in the case of 1335.8+2834 without extensive redshift data.

Hintzen, Romanishin & Valdes (1991) have also found significant clustering of galaxies around $z = 0.9$–1.5 radio-loud quasars. The galaxies responsible for the excess they detected seemed to be more luminous in the observed R-band than present-day brightest cluster galaxies. However, the galaxies responsible for the excess we have found in the field of 1335.8+2834 do not seem to be over-luminous in the K-band. Since the observed R-band samples ultraviolet light at these redshifts, evolutionary effects such as the presence of moderate amounts of young stars can boost up the observed flux considerably, while the NIR should show significantly milder evolutionary effects.

Excess in the galaxy number density has also been found for higher-redshift quasars or radio galaxies (Dressler et al. 1993, 1994; Hutchings 1995; Pascarelle et al. 1996). These authors claim that the excess galaxies are small compact objects which may be the 'building blocks' of today's luminous galaxies. In contrast, many of the galaxies found near 1335.8+2834 are fairly luminous ($\gtrsim 0.5L_*$). Similarly, an excess of $\sim L_*$ galaxies was found near radio-loud quasars at $z \sim 2$ by Aragón-Salamanca, Ellis, and O'Brien (1996). The situation is therefore not clear, and a systematic study of the fields of a large well-defined sample of known high redshift objects is clearly needed.

In summary, we have shown that the combination of deep optical and NIR imaging is a very powerful tool in revealing high redshift clusters of galaxies and/or their progenitors. Such clusters can provide samples of high redshift galaxies for evolutionary studies at large look-back times, which can greatly contribute to our knowledge of galaxy formation

and evolution at very early epochs. While this kind of study is very successful at finding candidate clusters, redshifts and morphologies will be ultimately needed.

This work was partially supported by a grant-in-aid for Scientific Research of the Japanese Ministry of Education, Science, Sports and Culture (No.07041104 and No.08740181). Part of this work was also supported by the Foundation for the Promotion of Astronomy of Japan. TY was a Special Post-Doctoral Researcher of the Institute of Physical and Chemical Research (RIKEN) and a part of this work was supported by this institute. AAS acknowledges generous financial support from the Royal Society and the Particle Physics and Astronomy Research Council. TK thanks to the Japan Society for the Promotion of Science Postdoctoral Fellowships for Research Abroad. KO was a visiting astronomer of the Institute for Astronomy, University of Hawaii and thanks their hospitality during his stay.

REFERENCES

Aragón-Salamanca, A., Ellis, R. S., Couch, W. J., & Carter, D. 1993, MNRAS, 262, 764

Aragón-Salamanca, A., Ellis, R.S. & O'Brien, K.S. 1996, MNRAS, 281, 945

Bessell, M. S. 1990, PASP, 102, 1181

Bower, R. G., Lucey, J. R., & Ellis, R. S. 1992, MNRAS, 254, 601

Dickinson, M. 1995, in ASP Conf. Ser. Vol.86 Fresh View of Elliptical Galaxies, eds. A. Buzzoni, A. Renzini, & A. Serrano, p.283

Dickinson, M. 1997a, in HST and the High Redshift Universe, ed. N. Tanvir, A. Aragón-Salamanca, and J.V. Wall, (Singapore: World Scientific), p.207

Dickinson, M. 1997b, in Galaxy Scaling Relations: Origins, Evolution and Applications, ed. L. da Costa (Springer-Verlag), in press, *astro-ph/9703035*

Dickinson, M. 1997c, in The Early Universe with the VLT, ed. J. Bergeron, (Springer-Verlag), p.274

Djorgovski, S. G., et al. 1995, ApJ, 438, L13

Dressler, A., & Smail, I. 1997, in HST and the High Redshift Universe, ed. N. Tanvir, A. Aragón-Salamanca, and J.V. Wall, (Singapore: World Scientific), p.185

Dressler, A., Oemler, A., Gunn, J., & Butcher, H. 1993, ApJ, 404, L45

Dressler, A., Oemler, A., Butcher, H., & Gunn, J. 1994, ApJ, 435, L23

Ellingson, E., & Yee, H. K. C. 1991, ApJ, 371, 49

Ellingson, E., Yee, H.K.C. & Green, R.F. 1991, ApJ, 371, 36

Ellis, R. S., Smail, I., Dressler, A., Couch, W. J., Oemler, A., Butcher, H., & Sharples, R. M. 1997, ApJ, 483, 582

Gregory, P.C., & Condon, J.J. 1991, ApJS, 75, 1011

Hintzen P., Romanishin W., & Valdes, F. 1991, ApJ, 366, 7

Hutchings, J. B. 1995, AJ, 110, 994

Hutchings, J. B., Crampton, D., & Persram, D. 1993, AJ, 106, 1324

Hutchings, J. B., Crampton, D., & Johnson, A. 1995, AJ, 109, 73

Jarvis, J. F., & Tyson, J. A. 1981, AJ, 86, 476

Johnson, H.L. 1966, ARA&A, 4, 193

Kodama, T., & Arimoto,N. 1997, A&A, 320, 41

Landolt, A. U. 1992, AJ, 104, 340

Pascarelle, S. M., Windhorst, R. A., Keel, W. C., & Odewahn, S. C. 1996, Nature, 383, 45

Smail, I., Hogg, D. W., Yan, L., & Cohen, J. G. 1995, ApJ, 449, L105

Stanford, S. A., Eisenhardt, P. R. M., & Dickinson, M. 1995, ApJ, 450, 512

Stanford, S.A., Eisenhardt, P.R.M., and Dickinson, M. 1997, ApJ, submitted

Véron-Cetty, M.-P. & Véron, P. 1996, A&AS, 115, 97

White, R. L., Becker, R. H., Helfand, D. J., Gregg, M. D. 1997, ApJ, 475, 479

Yamada T., & Arimoto, N. 1995, in IAU symp. No.171, New Light on Galaxy Evolution, eds. R. Bender, & R. L. Davies, p.472

Yee, H. K. C. & Green, R. F. 1987, ApJ, 319, 28

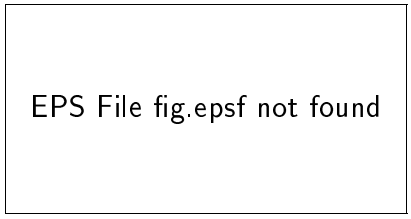

Fig. 1.— *RIK* three color image of the field near the radio-loud quasar 1335.8+2834 at $z = 1.086$ (QSO). North is up, East is left. The field is 160 arcsec on each side, which corresponds to $0.62\,h^{-1}$Mpc for q_0=0.5.

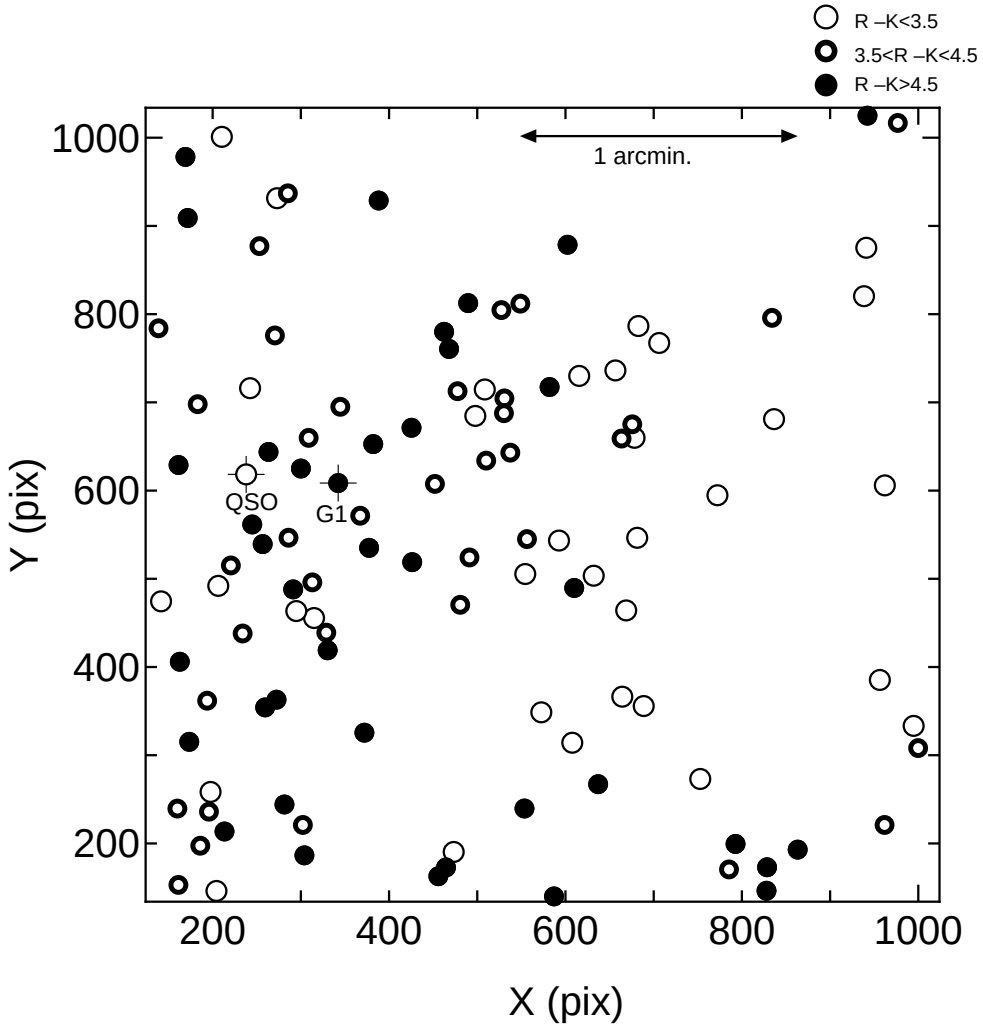

Fig. 2a.— **(a)** Distribution of the K-selected objects on the sky. Scale and orientation as in Figure 1. Objects in different color ranges are shown as different symbols.

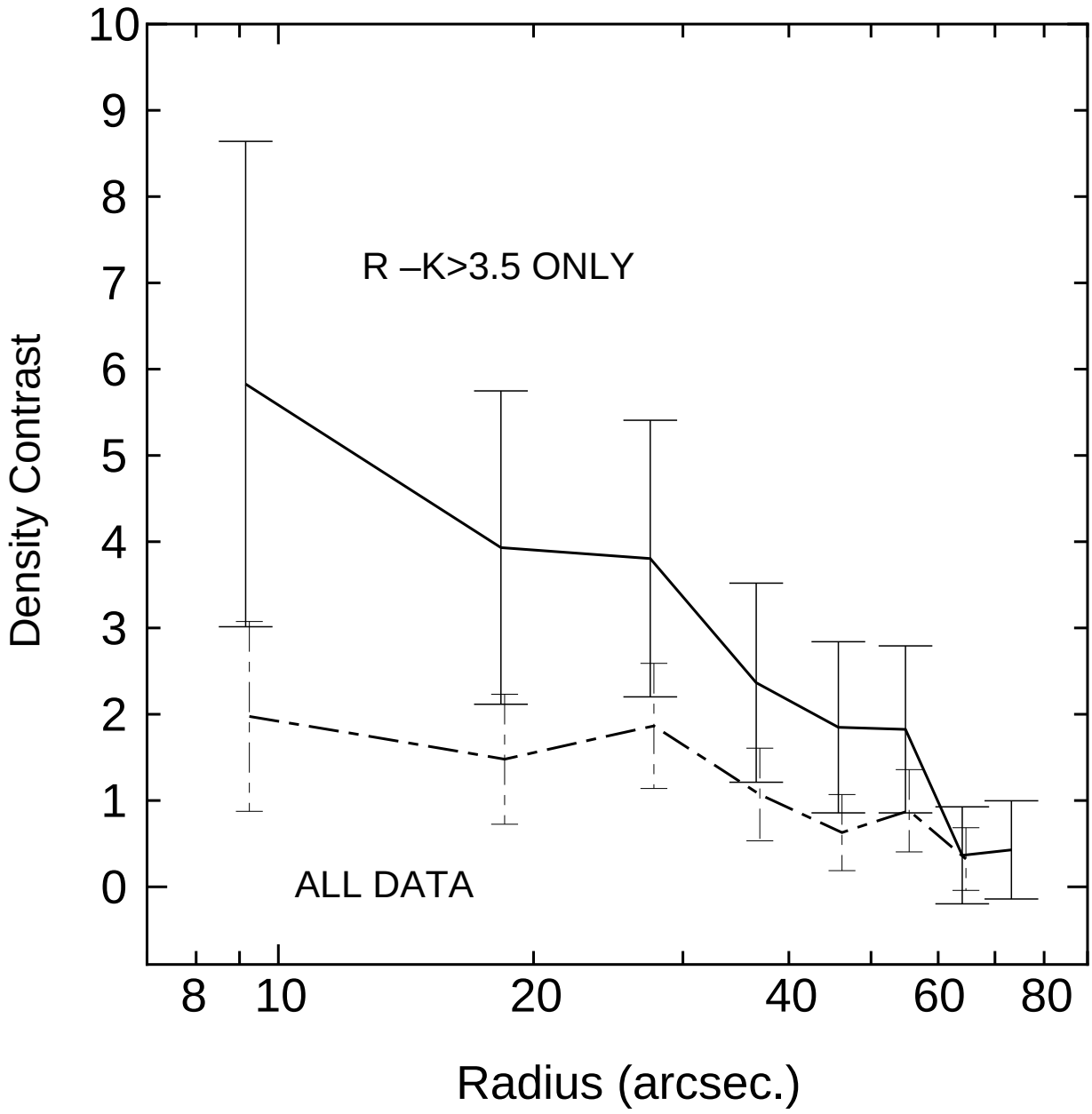

Fig. 2b.— **(b)** Surface-density-contrast profile, $(\Sigma(\theta)-\langle\Sigma\rangle)/\langle\Sigma\rangle$, for all the K-selected objects centered on galaxy G1 (dash-dotted line) and for the objects with $R-K \geq 3.5$ (solid line). The average field number densities are the values obtained at the western half of the image avoiding the cluster region.

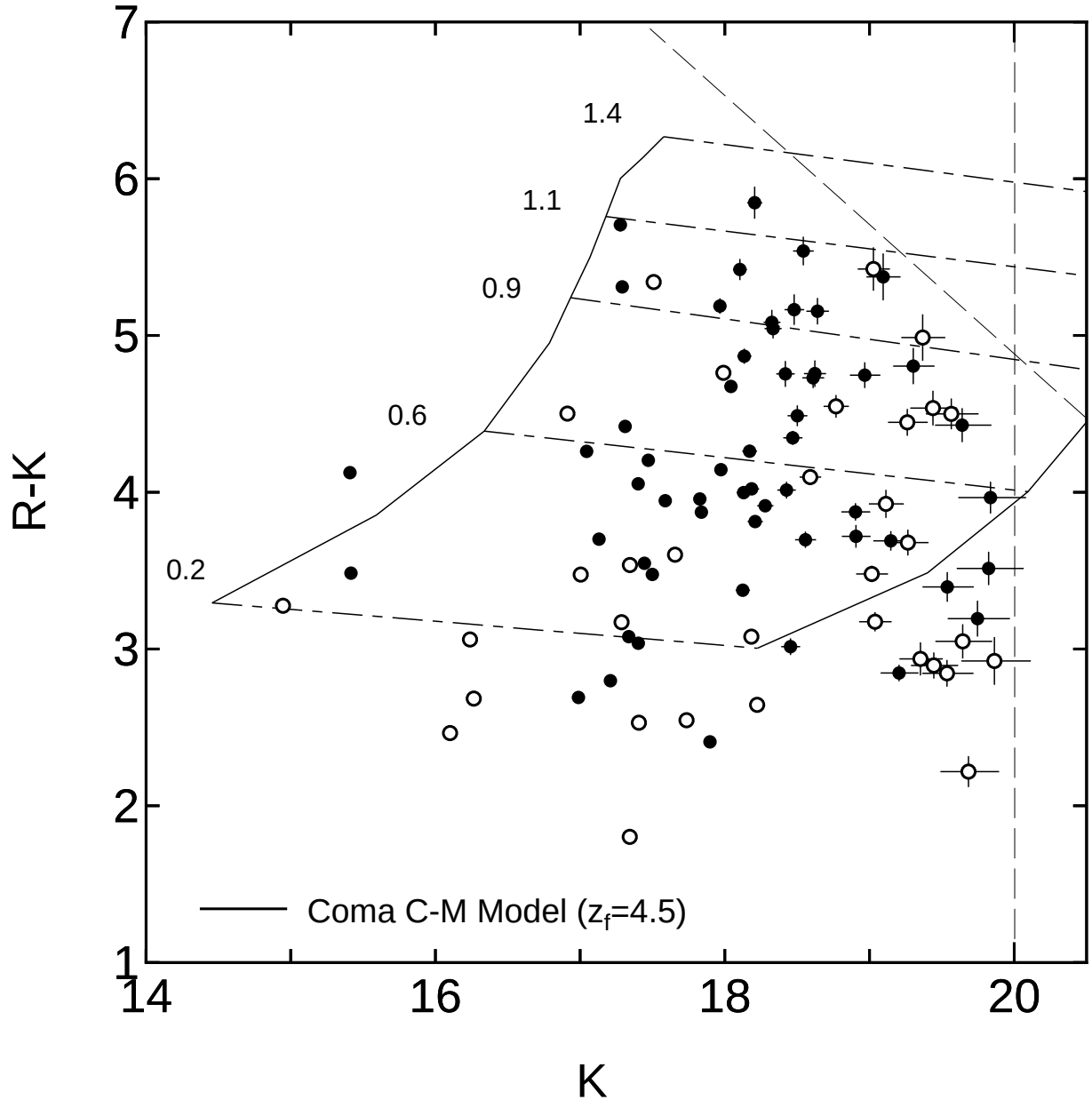

Fig. 3.— $R-K$ vs. K color-magnitude diagram of the complete photometric sample. The completeness limits are shown by the dashed lines. The objects in the putative cluster region, namely the eastern half of the frame, are shown as filled circles. Those in the western half are shown as open circles. The predicted colors and magnitudes of model galaxies with $M_V = -22.0$ and -18.5 mag at $z = 0$, formed at $z_f = 4.5$ are shown as solid lines. Tilted dash-dotted lines indicate the expected color-magnitude relation observed at $z = 0.2$, 0.6, 0.9, 1.1, and 1.4, which correspond to galaxy ages of 8.9, 5.4, 3.9, 3.2, and 2.5 Gyr, respectively (computed from the models of Kodama and Arimoto 1997).

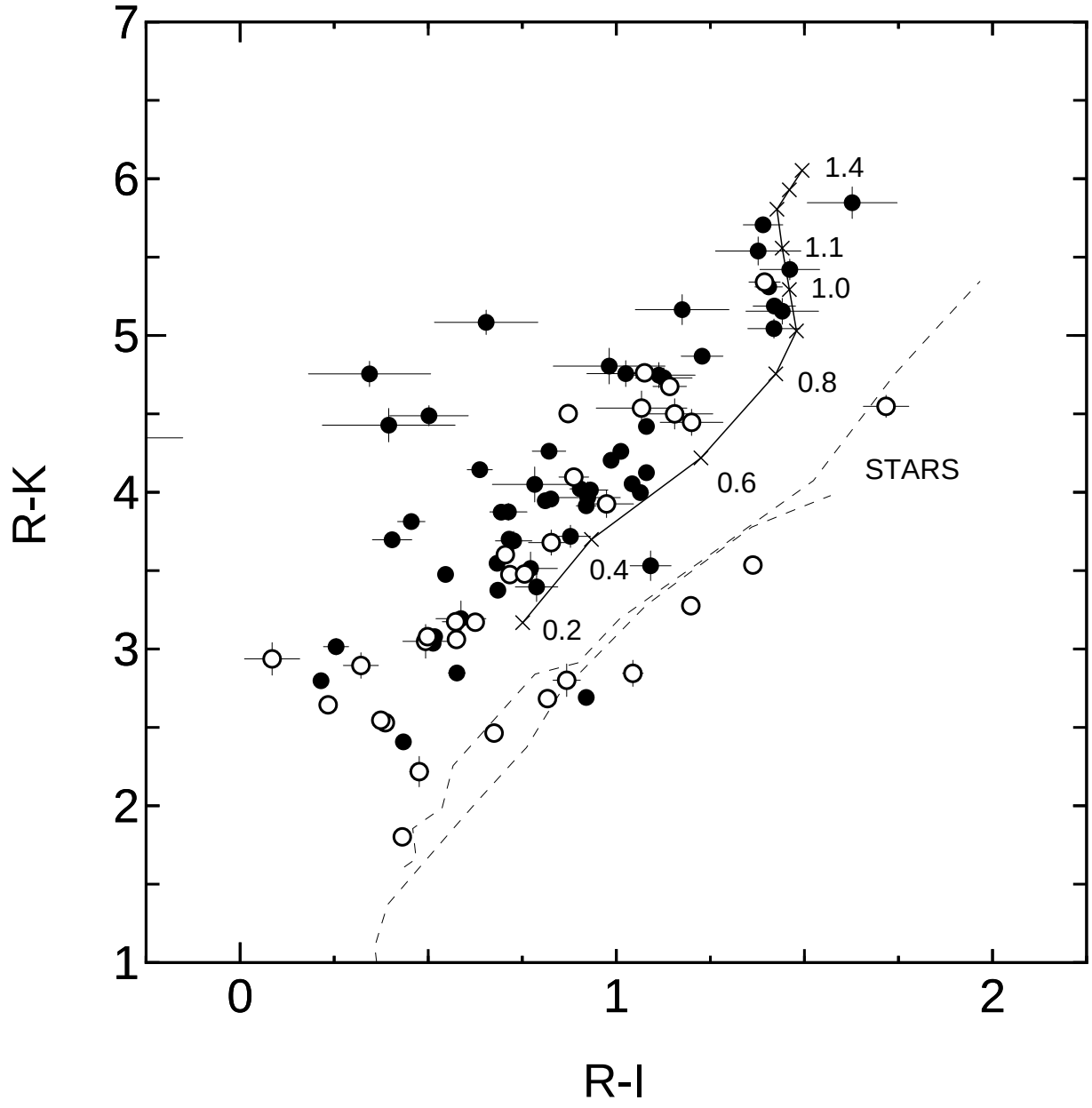

Fig. 4.— $R-K$ vs. $R-I$ color-color diagram for the complete sample. Symbols are as in Figure 3. The solid line indicates the predicted colors of model galaxies with $M_V = -20.5$ mag at $z = 0$ observed at various redshifts derived from the same models as in Figure 3. The labeled crosses indicate the observed redshifts. Colors of dwarf (G0V–M5V) and giant (G5III–M6III) stars (Johnson 1966; Bessell 1990) are also plotted for reference (dashed lines).

This figure "hzell_fig1.gif" is available in "gif" format from:

http://arXiv.org/ps/astro-ph/9707197v1

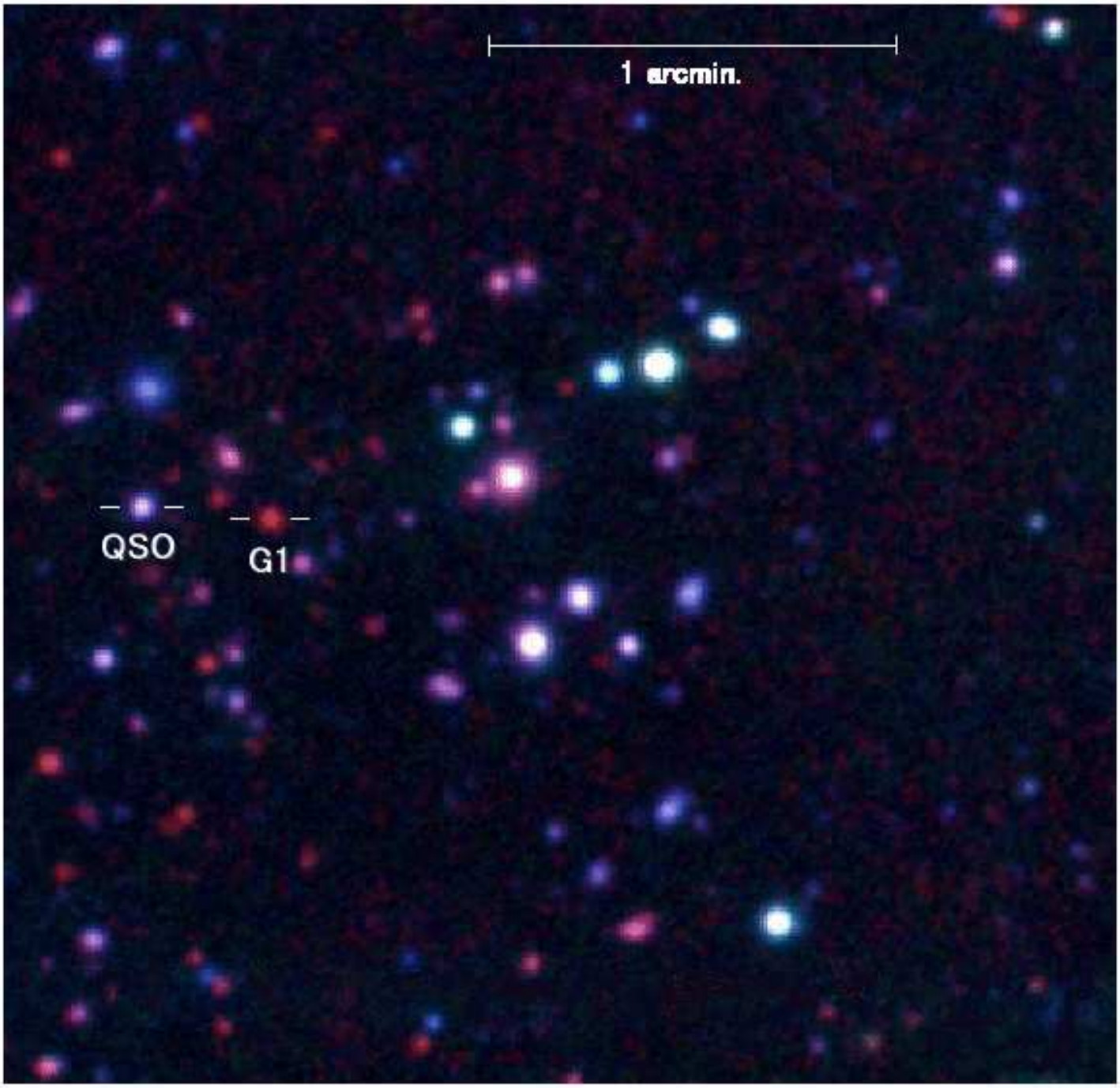
1 arcmin.
QSO
G1

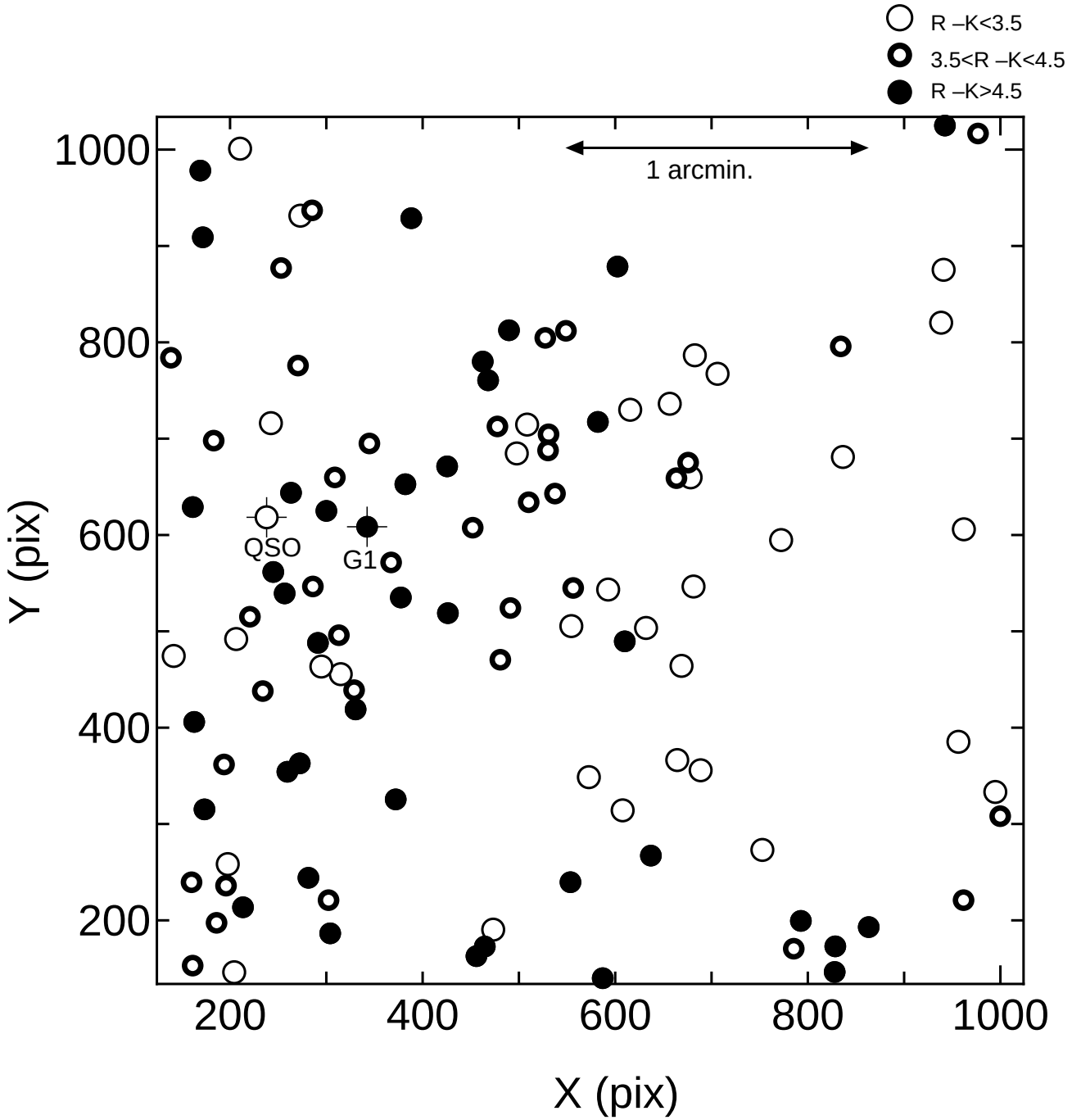
R –K<3.5
3.5<R –K<4.5
R –K>4.5
1 arcmin.
QSO
G1
1000
800
600
400
200
Y (pix)
200
400
600
800
1000
X (pix)

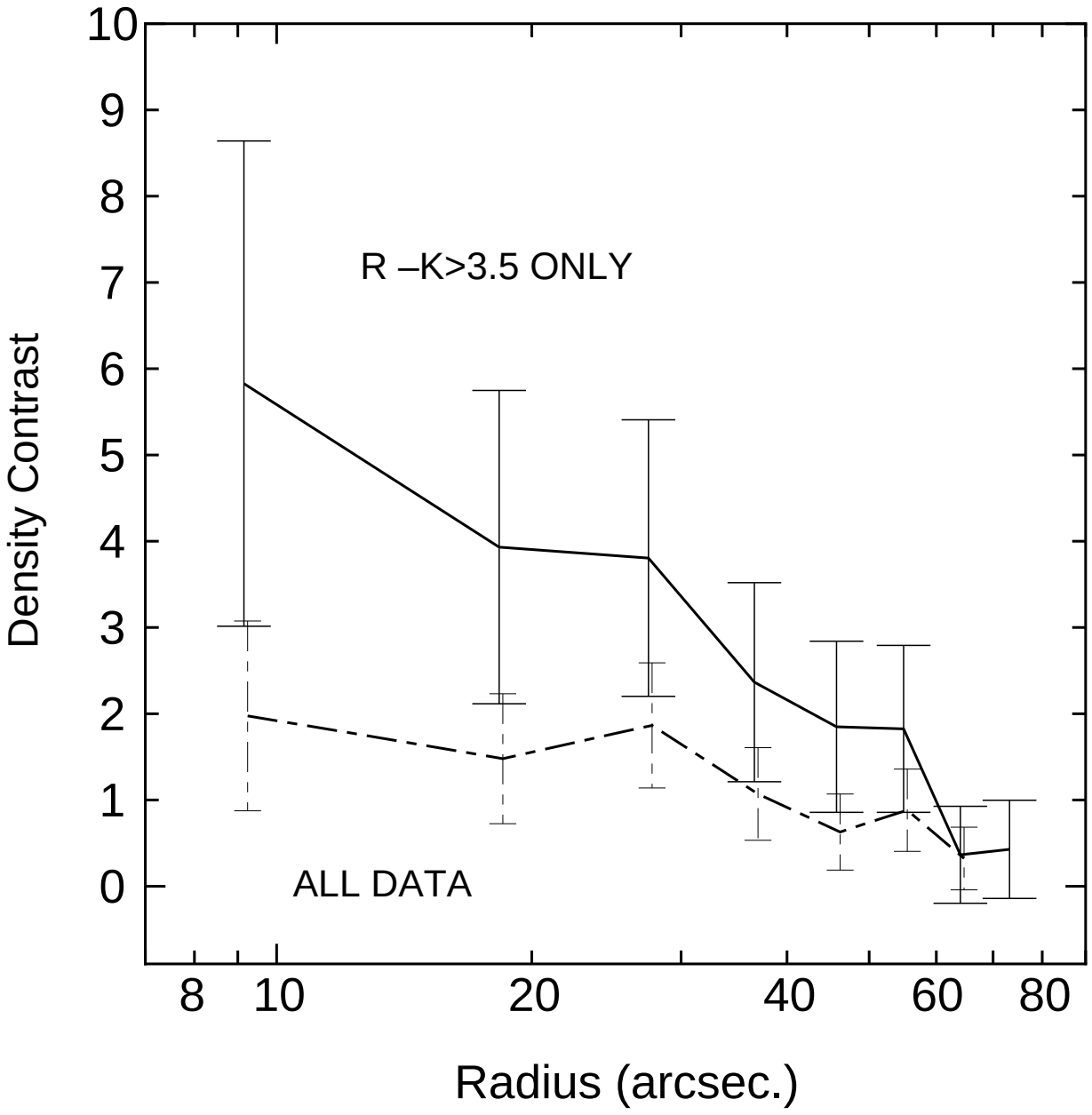
10
9
8
7
6
5
4
3
2
1
0
Density Contrast
R –K>3.5 ONLY
ALL DATA
8
10
20
40
60
80
Radius (arcsec.)

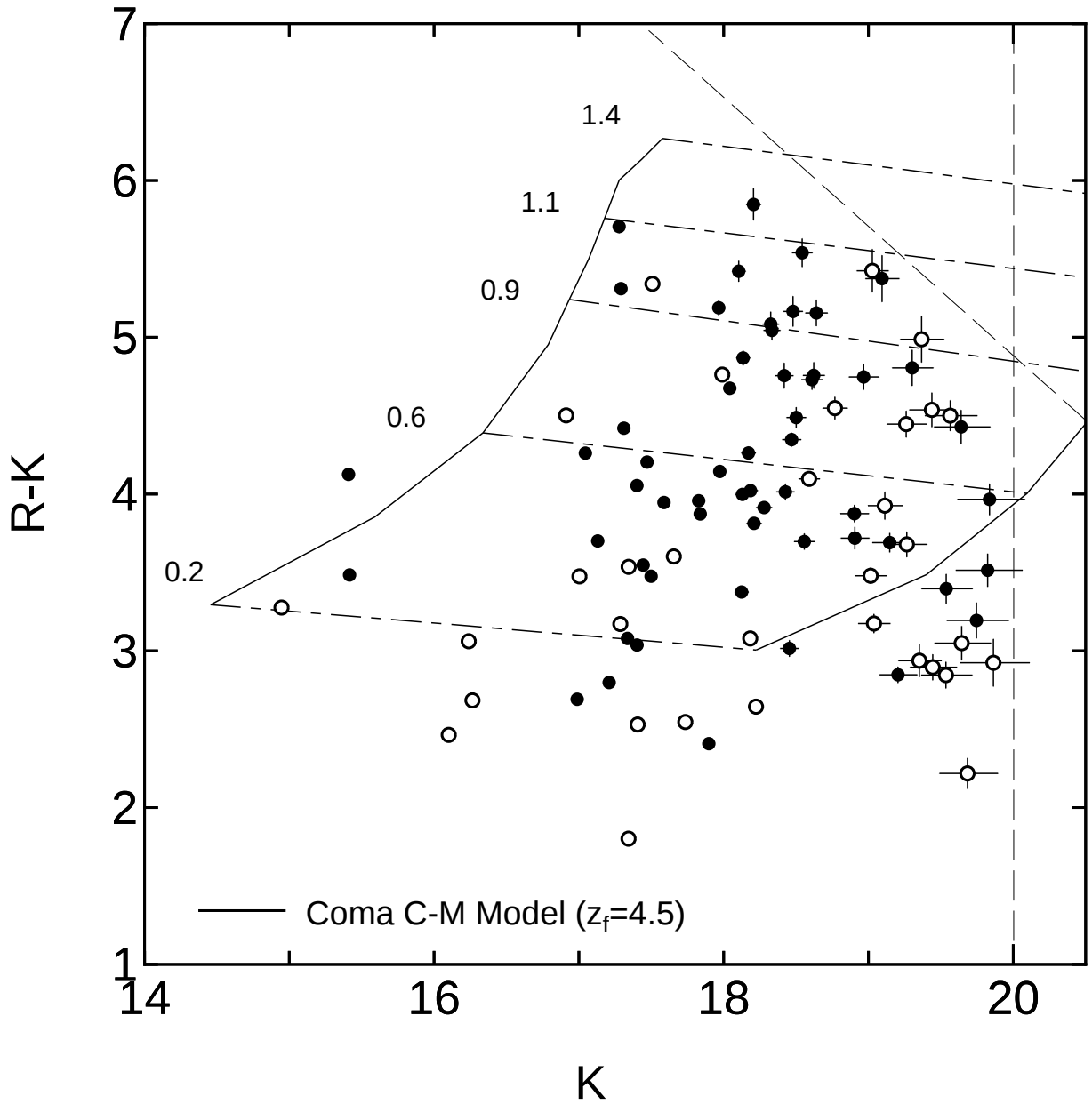
7
6
5
4
3
2
1
14
16
18
20
R-K
K
1.4
1.1
0.9
0.6
0.2
Coma C-M Model (z_f=4.5)

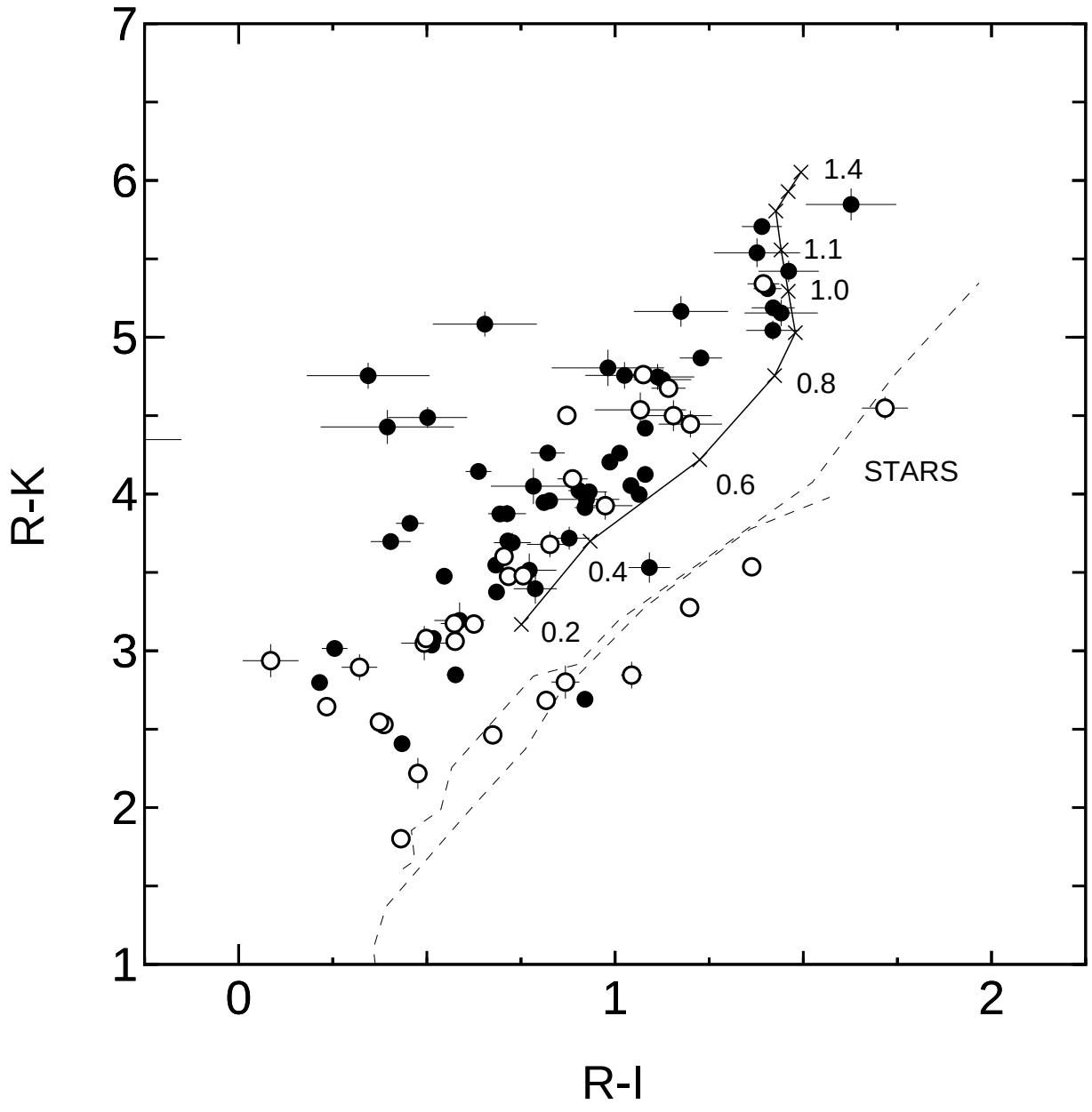
7
6
5
4
3
2
1
0
1
2
R-K
R-I
1.4
1.1
1.0
0.8
0.6
0.4
0.2
STARS